

International Journal of Modern Physics A  
 © World Scientific Publishing Company

## Extra-dimensional models on the lattice

Francesco Knechtli

*Department of Physics, Bergische Universität Wuppertal  
 Gausstr. 20, D-42119, Wuppertal, Germany  
 knechtli@physik.uni-wuppertal.de*

Enrico Rinaldi

*Nuclear and Chemical Sciences Division  
 Lawrence Livermore National Laboratory  
 Livermore, CA 94550, USA  
 rinaldi2@llnl.gov*

Received 13 May 2016

In this review we summarize the ongoing effort to study extra-dimensional gauge theories with lattice simulations. In these models the Higgs field is identified with extra-dimensional components of the gauge field. The Higgs potential is generated by quantum corrections and is protected from divergencies by the higher dimensional gauge symmetry. Dimensional reduction to four dimensions can occur through compactification or localization. Gauge-Higgs unification models are often studied using perturbation theory. Numerical lattice simulations are used to go beyond these perturbative expectations and to include non-perturbative effects. We describe the known perturbative predictions and their fate in the strongly-coupled regime for various extra-dimensional models.

WUB/16-01, LLNL-JRNL-691819

*Keywords:* lattice simulations; extra dimensions; gauge-Higgs unification; symmetry breaking

### 1. Gauge-Higgs unification: a scalar from extra dimensions

The Higgs sector of the Standard Model is the only one containing an elementary scalar field. After the discovery of the Higgs boson<sup>1,2</sup> and the measurements of its couplings at the LHC in recent years, we know that the Higgs sector is a remarkably good effective description of low-energy electro-weak physics. However, we would like to explain why the Higgs mass is so light and we would like to know if the spontaneous symmetry breaking (SSB) mechanism described by Brout, Englert and Higgs<sup>3-5</sup> has a more profound origin, maybe from a more complete theory at high energy. The recent observation of a diphoton excess in the scalar channel at about 750 GeV at the ATLAS and CMS experiments,<sup>6,7</sup> if confirmed, will find no explanation within the Standard Model, bringing forth the need for a more general theory.

2 *F. Knechtli and E. Rinaldi*

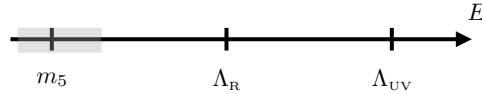


Fig. 1. The figure shows the desired separation of energy scales in a five-dimensional theory with cutoff  $\Lambda_{UV}$  and compactification scale  $\Lambda_R = \frac{1}{2\pi R}$ . The shaded area is the region where we expect the scalar mass  $m_5$  to be described by Eq. (1).

Intriguingly, the existence of hidden extra dimensions<sup>8,9</sup> can address both the lightness of the Higgs and the origin of SSB, while providing a natural framework for the unification of gauge forces. The idea that the Higgs field may be directly related to the components of extra-dimensional gauge fields was first discussed in Ref. 10 and it is the foundational concept thorough all the models we discuss in this review.

Five-dimensional Yang–Mills theories compactified on a circle have a light scalar mode, whose mass renormalization  $m_5$  in perturbation theory is protected by the remnant of the higher-dimensional gauge symmetry.<sup>11–17</sup> The extra-dimensional gauge theory is naively non-renormalizable and is regulated with a cutoff  $\Lambda_{UV}$ , which interestingly does not affect the quantum corrections to the scalar mass at one loop:

$$m_5^2 = \frac{9g_5^2 N_c}{32\pi^5 R^3} \zeta(3), \quad (1)$$

where  $g_5$  is the five-dimensional gauge coupling and  $\zeta$  is the Riemann Zeta-function.<sup>a</sup>

This relation is true if the details of the regularization can be neglected at the scale of compactification,  $\Lambda_R \sim R^{-1} \ll \Lambda_{UV}$ , but its validity is restricted to the weak-coupling region. Lattice simulations are able to access non-perturbative physics, and numerically investigate the theory in the regime where the hierarchy of scales is such that the low-energy physics is described by a four-dimensional effective theory with a light scalar particle and check if Eq. (1) holds. The desired separation of scales is pictorially shown in Fig. 1. This scenario is summarized in Sec. 3.

The scalar particle that is present in the dimensionally reduced theory is in the same representation of the gauge group as the extra-dimensional gauge field. Therefore, the compactification mechanism broadly described above for a pure gauge theory will provide an adjoint scalar, which can not describe the Higgs particle. A fundamental scalar can be obtained if the extra dimension is compactified on an orbifold instead of a circle. This scenario is reviewed in Sec. 5 and has the additional advantage to provide a description for chiral fermions from an extra dimension.

<sup>a</sup> Eq. (1) applies to a circular extra dimension. If it is an interval (orbifold), there is an extra factor  $1/2$ .

In perturbation theory, Eq. (1) arises from an effective potential that is generated by radiative correction. This effective potential has a trivial minimum in a Yang–Mills theory, but is modified by the addition of fermions in the adjoint or in the fundamental representation. The fermionic effects destabilize the trivial minimum and a vacuum that breaks the gauge symmetry is possible. This is the basis of the Hosotani mechanism<sup>11</sup> whose non-perturbative application is explored in Sec. 4. There exists an alternative non-perturbative mechanism of spontaneous gauge symmetry breaking. It takes place on the orbifold (but not on the torus) and relies on the SSB of a global symmetry in accordance with Elitzur’s theorem.<sup>18</sup> This will be discussed in Sec. 5.

Dimensional reduction to four dimensions can occur if the extra dimension becomes compact. This is the Kaluza–Klein mechanism. Another mechanism is localization. In flat space localization can be realized in a way similar to the layered phase.<sup>19</sup> At present, the searches that the LHC performs for discovering extra dimensions are connected to the compactification scenario. It is possible that if there exists an extra dimension with an underlying localization mechanism at work, the experimental signatures may be different.

The review is structured as follows. In Sec. 2 we introduce the general setting used to study extra-dimensional models on the lattice by numerical Monte Carlo simulations and in mean-field analytical calculations that we also introduce in the same section. Sec. 3 is devoted to a summary of results for Yang–Mills theories in more than four dimensions with toroidal boundary conditions. Then we discuss theories with fermions and the accompanying Hosotani mechanism in Sec. 4. Finally, we report the results of the study of Yang–Mills theories with orbifold boundary conditions and the non-perturbative realization of gauge-Higgs unification in Sec. 5.

We do not discuss extra-dimensional supersymmetric models or the importance of extra dimensions in string theories and other theories of gravity. Lattice studies in those directions are covered by other reviews of this series (Supersymmetry and Gauge/Gravity duality).

## 2. Extra-dimensional gauge theories on the lattice

Lattice methods are useful to investigate the phase diagram of extra-dimensional gauge theories and to study the non-perturbative viability of various mechanisms for dimensional reduction. In order to have a self-contained description, in this section we summarize different geometries studied on the lattice and, in later sections, we will describe their emerging properties and phase diagrams.

### 2.1. *Torus geometry*

The original mathematical idea of extra dimensions<sup>8,9</sup> relies on the existence of a compactification radius  $R$ . On a torus geometry, where periodic boundary conditions for the gauge fields are imposed in all directions, compactification can be easily

4 *F. Knechtli and E. Rinaldi*

achieved by reducing the size of the extra dimension  $L_5 = 2\pi R$  below a critical value  $L_{5c}$  and keeping the other dimensions large.

It is rather straightforward to study this compactified theory on the lattice. As a first step we discretize the continuum five-dimensional Euclidean action using the Wilson plaquette action. For an  $SU(N_c)$  gauge theory on the torus this is given by<sup>20</sup>

$$S_W^{tor} = \sum_{n_\mu} \sum_{n_5=0}^{N_5-1} \left[ \frac{\beta_4}{N_c} \sum_{\mu < \nu} \text{Re Tr} \{1 - U_{\mu\nu}(n_\mu, n_5)\} + \frac{\beta_5}{N_c} \sum_{\mu} \text{Re Tr} \{1 - U_{\mu 5}(n_\mu, n_5)\} \right], \quad (2)$$

where  $\beta_4$  and  $\beta_5$  denote the lattice coupling in the four standard dimensions and in the fifth (extra) dimension respectively,  $U_{MN}(n_\mu, n_5)$  with  $M, N = 0, 1, 2, 3, 5$  is the plaquette in directions  $M$  and  $N$  located on lattice site indexed by  $n_\mu$  in the four standard dimensions and  $n_5$  in the extra dimension. This is a standard choice.<sup>21–26</sup>

The action Eq. (2) with the lattice couplings  $\beta_4$  and  $\beta_5$  allows for different lattice spacings  $a_4$  and  $a_5$ , where  $a_4$  denotes the lattice spacing in the usual four dimensions and  $a_5$  denotes the lattice spacing in the extra dimension. This is naturally suited for choosing the size of the extra dimension  $L_5 = 2\pi R = N_5 a_5$  independently from the size of the four dimensional space-time  $L = N_4 a_4$ . Here  $N_4$  and  $N_5$  are the number of lattice points in each of the four directions and in the fifth direction, respectively.

An equivalent parametrization for Eq. (2) uses  $\beta = \sqrt{\beta_4 \beta_5}$  and  $\gamma = \sqrt{\beta_5 / \beta_4}$ . In the classical limit  $(a_4, a_5) \rightarrow 0$

$$\gamma = \frac{a_4}{a_5} \quad \text{and} \quad \beta = \frac{2N_c a_4}{g_5^2}, \quad (3)$$

where  $g_5$  is the dimensionful continuum gauge coupling. Therefore,  $\gamma$  is often called the *anisotropy* coefficient, giving a tree-level prediction for the ratio of lattice spacings. The non-perturbative anisotropy  $\xi$  can be directly measured by looking at ratios of lattice correlation functions.<sup>27</sup>

The regime where  $\gamma > 1$  is clearly associated with a small spacing in the extra dimension  $a_5$  compared to  $a_4$ . The size of the extra dimension with respect to the four-dimensional lattice spacing can be written as  $\tilde{N}_5 = N_5 / \gamma$ . On the other hand, the regime where  $\gamma < 1$  is associated with a larger lattice spacing along the extra dimension than in the four-dimensional hyperplanes orthogonal to it. In the limit  $\beta_5 = 0$  the action Eq. (2) describes  $N_5$  independent copies of four-dimensional gauge theories on the hyperplanes. The regime at  $\gamma < 1$  is connected with this limit.

As a second step in the study of extra-dimensional theories on the lattice, different values for dimensions  $(L, L_5)$  and the gauge coupling  $g_5^2$  of the continuum theory can be probed by modifying the parameters of the lattice model  $(N_4, N_5, \beta_4, \beta_5)$ . In the lattice model's parameter space, physical properties of the low energy regime of

the theory, such as a mass gap or the static potential, are studied with traditional lattice methods described in the Introduction by the editors.

We should note that five-dimensional gauge theories are perturbatively non-renormalizable, due to the negative mass dimension of the gauge coupling  $g_5$ . In the continuum if the cutoff of the theory is infinite the coupling is necessarily zero. On the lattice the cutoff is given by the inverse lattice spacing  $a_4^{-1}$ . The only continuum limit  $a_4 \rightarrow 0$ , which is known to exist so far, is the perturbative trivial limit. Triviality can also be understood by considering the one-loop renormalization of the effective four-dimensional coupling  $g_4^2 = g_5^2/(N_5 a_5)$ .<sup>28,29</sup>

## 2.2. Orbifold geometry

The orbifold theory we consider here is defined in the five-dimensional domain  $I = \{n_\mu, 0 \leq n_5 \leq N_5\}$  with volume  $N_t \times N_s^3 \times N_5$ . The Wilson action for an  $SU(N_c)$  gauge theory on this orbifold is given by<sup>30,31</sup>

$$S_W^{orb} = \sum_{n_\mu} \left[ \frac{\beta_4}{N_c} \sum_{n_5=0}^{N_5} \sum_{\mu < \nu} w \operatorname{Re} \operatorname{Tr} \{1 - U_{\mu\nu}(n_\mu, n_5)\} + \frac{\beta_5}{N_c} \sum_{n_5=0}^{N_5-1} \sum_{\mu} \operatorname{Re} \operatorname{Tr} \{1 - U_{\mu 5}(n_\mu, n_5)\} \right], \quad (4)$$

which follows the parametrization of Eq. (2). The weight  $w$  is due to the orbifold geometry and is set to  $\frac{1}{2}$  for plaquettes on the boundary and 1 elsewhere. Lattice gauge fields on the orbifold obey the boundary conditions

$$U_\mu(n_\mu, n_5) = g U_\mu(n_\mu, n_5) g^{-1}, \quad \text{for } n_5 = 0, N_5. \quad (5)$$

The matrix  $g$  is an element of  $SU(N_c)$  such that  $g^2$  is in the center  $\mathbb{Z}_{N_c}$  of  $SU(N_c)$ . The boundary conditions Eq. (5) break in general the gauge group  $SU(N_c)$  down to a subgroup  $H$  on the orbifold boundaries according to the pattern  $SU(p+q) \rightarrow SU(p) \times SU(q) \times U(1)$  (see for example Ref. 32). As an example, for gauge group  $SU(2)$  the choice  $g = -i\sigma^3$  breaks the gauge group to  $U(1)$  on the orbifold boundaries.

The operators representing the scalar and vector particles on the orbifold are defined as follows. The left-to-right boundary-to-boundary-line is denoted by  $l(n_\mu) = \prod_{n_5=0}^{n_5=N_5-1} U_5(n_\mu, n_5)$ . Starting from the Polyakov loop on the torus, its orbifold projection yields  $p = l g l^\dagger g^\dagger$ , which is a field living on the left boundary (an analogous field living on the right boundary can also be defined). Scalar operators can be defined as

$$\mathcal{P} = \operatorname{tr} (p) \quad \text{or} \quad \mathcal{H} = \operatorname{tr} (h h^\dagger) \quad (6)$$

using for  $h$  the expression

$$h(n_\mu) = \frac{1}{4N_5} [p(n_\mu) - p^\dagger(n_\mu), g]. \quad (7)$$

6 *F. Knechtli and E. Rinaldi*

Vector gauge boson operators can be defined as

$$\mathcal{Z}(n_\mu) = \text{tr} \left( g U_k(n_\mu, n_5 = 0) h(n_\mu + \hat{k}) U_k(n_\mu, n_5 = 0)^\dagger h(n_\mu) \right). \quad (8)$$

These operators were introduced in Ref. 33.

The theory defined by Eq. (4) possesses a global stick symmetry,  $\mathcal{S}$ .<sup>34</sup> This symmetry is defined by the combination  $\mathcal{S} = \mathcal{S}_L \cdot \mathcal{S}_R$ , where  $\mathcal{S}_L$  is a symmetry defined on the left boundary via

$$U_5(n_5 = 0) \rightarrow g_s^{-1} U_5(n_5 = 0) \quad \text{and} \quad U_\nu(n_5 = 0) \rightarrow g_s^{-1} U_\nu(n_5 = 0) g_s. \quad (9)$$

(We suppress here the coordinate  $n_\mu$ .) The symmetry  $\mathcal{S}_L$  is generated by an element  $g_s$  with  $\{g, g_s\} = 0$ , which is not a gauge or center transformation.  $g_s$  is an element of the generalized Weyl group,  $W_{\text{SU}(N_c)}(H) = N_{\text{SU}(N_c)}(H)/H$ , which is the coset of the normalizer of  $H$  in  $\text{SU}(N_c)$  divided by  $H$ .<sup>35</sup> As an example, for the  $\text{SU}(2)$  orbifold with  $g = -i\sigma^3$ , a stick matrix is  $g_s = -i\sigma^1$ .  $\mathcal{S}_R$  can be defined on the right boundary in an equivalent fashion.

$$U_5(n_5 = N_5 - 1) \rightarrow U_5(n_5 = N_5 - 1) g_s \quad \text{and} \quad U_\nu(n_5 = N_5) \rightarrow g_s^{-1} U_\nu(n_5 = N_5) g_s. \quad (10)$$

The scalar operators in Eq. (6) are invariant under the stick symmetry  $\mathcal{S}$  while the gauge boson operator in Eq.(8) is odd under this symmetry. This latter property plays an important role as we will see in Sec. 5.2.

### 2.3. Mean-field approach

The mean-field approach to lattice gauge theory is reviewed in Ref. 36. We briefly introduce it here. The link variables  $U$  in  $\text{SU}(N_c)$  are traded for the unconstrained complex variables  $V$  and the Lagrange multipliers  $H$  used to represent the  $\delta$  functions  $\delta(V - U)$ . The partition function for gauge action  $S_W$  can be rewritten as

$$Z = \int \mathcal{D}[V] \int \mathcal{D}[H] e^{-S_{\text{eff}}[V, H]},$$

$$S_{\text{eff}} = S_W[V] + \sum_{n, M} [u(H_M(n)) + (1/N_c) \text{Re tr} \{H_M(n) V_M(n)\}] \quad (11)$$

where the effective mean-field action  $u(H)$  for a given link  $U_M(n)$  is defined via

$$e^{-u(H)} = \int dU_M(n) e^{(1/N_c) \text{Re tr} \{U_M(n) H\}}. \quad (12)$$

The mean-field or zeroth order approximation amounts to finding the minimum of the effective action. On a periodic isotropic lattice the variables  $V$  and  $H$  are set proportional to the unit matrix,  $H = \bar{H} \mathbf{1}$  and  $V = \bar{V} \mathbf{1}$ . The zeroth order saddle point solution or "mean-field background"  $\bar{H}$  and  $\bar{V}$  can be easily obtained by taking derivatives of  $S_{\text{eff}}$  in Eq. (11) with respect to  $V$  and  $H$  and require them to vanish. Gaussian fluctuations are defined by setting  $H = \bar{H} + h$  and  $V = \bar{V} + v$ . For the calculation of corrections stemming from fluctuations gauge fixing is necessary.

Covariant gauge fixing on  $v$  is a practical choice. In Ref. 37 it was shown that this is equivalent to gauge-fix the original links  $U$ . We denote the quadratic part of the effective action by

$$S^{(2)}[v, h] = \frac{1}{2} \left[ h^T K^{(hh)} h + 2v^T K^{(vh)} h + v^T (K^{(vv)} + K^{(\text{gf})}) v \right], \quad (13)$$

where  $K^{(\text{gf})}$  is the contribution from the gauge fixing term. The expectation value  $\langle \mathcal{O}(U) \rangle$  of an observable  $\mathcal{O}$  to first order in the mean-field expansion is given by

$$\langle \mathcal{O} \rangle = \mathcal{O}[\bar{V}] + \frac{1}{2} \text{tr} \left\{ \frac{\delta^2 \mathcal{O}}{\delta V^2} \Big|_{\bar{V}} K^{-1} \right\}, \quad (14)$$

where the propagator  $K$  is defined as

$$K = - \left( K^{(hh)} \right)^{-1} + K^{(vv)} + K^{(\text{gf})} \quad (15)$$

and the second derivative of the observable is evaluated in the mean-field background. Masses are calculated by evaluating the connected two point point function  $C(t)$  of a time dependent observable  $\mathcal{O}(t)$  in the mean-field expansion. To first order in the fluctuations the expression reduces to  $C(t) = C^{(1)}(t)$  with

$$C^{(1)}(t) = \frac{1}{2} \text{tr} \left\{ \frac{\delta^{(1,1)} \mathcal{O}(t_0 + t) \mathcal{O}(t_0)}{\delta^2 V} K^{-1} \right\}, \quad (16)$$

where the notation  $\delta^{(1,1)}$  means one derivative acting on each of the  $\mathcal{O}(t_0 + t)$  and  $\mathcal{O}(t_0)$ . The mass of the lowest lying state is then  $m = \lim_{t \rightarrow \infty} \ln \frac{C^{(1)}(t)}{C^{(1)}(t-1)}$ .

Caveats of the mean-field are the gauge dependence of the background, the lack of guarantee that the expansion converges and the appearance of fake phase transitions. Concerning the gauge dependence, physical observables are found to be independent on the gauge fixing for the class of gauges considered in Refs. 22,38. The mean-field corrections come multiplied by powers of  $1/d$  (where  $d$  is the number of dimensions) and therefore convergence is expected to become better as the number of dimensions increases. In order to check for the possibility of mean-field artifacts it is crucial to perform Monte Carlo simulations. As we will see in Sec. 3.4 and 5.1, it turns out that the mean-field in five dimensions captures the qualitative properties (like dimensional reduction or spontaneous symmetry breaking) of the system.

### 2.3.1. Mean-field on the torus

We present a quick way to determine the mean-field background. The starting point are the link averages. In the case of  $\text{SU}(2)$  the link average is defined by (see for example Ref. 39)

$$\langle U \rangle = \frac{\int_{\text{SU}(2)} dU U e^{\frac{1}{2} \text{tr}(UB^\dagger)}}{\int_{\text{SU}(2)} dU e^{\frac{1}{2} \text{tr}(UB^\dagger)}} = V \frac{I_2(b)}{I_1(b)}, \quad (17)$$

8 *F. Knechtli and E. Rinaldi*

where  $B = bV$ ,  $b \in \mathbb{R}$  and  $V \in \text{SU}(2)$ . The matrix  $B$  originates from the gauge action and is equal, up to a factor, to the sum of the staples. In the case of  $\text{U}(1)$  the link average gives (cf. Ref. 38)

$$\langle U \rangle = \frac{\int_{\text{U}(1)} dU U e^{\text{Re}(UB^*)}}{\int_{\text{U}(1)} dU e^{\text{Re}(UB^*)}} = V \frac{I_1(b)}{I_0(b)}, \quad (18)$$

where  $B = bV$ ,  $b \in \mathbb{R}$  and  $V \in \text{U}(1)$ .

Consider the case of  $\text{SU}(2)$  on a  $d$  dimensional torus. The action is a generalization of Eq. (2) to  $d$  dimensions where we set  $\beta_4 = \beta_5$ . The mean-field background is parametrized by the mean-link  $U = u \times \mathbf{1}_2$ . The consistency condition that the link average Eq. (17) is equal to the mean-link, yields the relation

$$b = 2(d-1)\beta u^3, \quad u = \frac{I_2(b)}{I_1(b)}. \quad (19)$$

It can be easily solved by numerical iteration.

The generalization of Eq. (19) to the anisotropic gauge action is given in Ref. 22, where the five-dimensional  $\text{SU}(2)$  gauge theory is considered. There explicit formulae for the calculation of the scalar and gauge boson masses as well as for the static potential including fluctuations at leading order are presented.

### 2.3.2. Mean-field on the orbifold

On the orbifold translation invariance is broken. The mean-links are set to

$$\begin{aligned} U_\mu(n) &= u(n_5) \times \mathbf{1}_2, & n_5 &= 0, \dots, N_5 \\ U_5(n) &= u(n_5 + 1/2) \times \mathbf{1}_2, & n_5 &= 0, \dots, N_5 - 1 \end{aligned}$$

Equating each link to its link average yields a system of equations<sup>31,38</sup> which can be solved by numerical iteration. The link averages for the  $\text{U}(1)$  boundary links are computed using Eq. (18) and for the  $\text{SU}(2)$  links using Eq. (17).

On the orbifold the calculation of the inverse propagator in Eq. (15) is complicated by the breaking of translational invariance. This calculation is presented in Ref. 38. There explicit formulae for the calculation of the scalar and gauge boson masses as well as for the static potential including fluctuations at leading order are also presented.

## 2.4. Other models

In this section we present other models where five-dimensional gauge theories have been studied. The first is a formulation of these theories with a warped metric to study gauge field localization. The second is a Lifshitz-type anisotropic formulation to study the possibility to take a continuum limit.

Motivated by the Randall-Sundrum model<sup>40,41</sup> to localize gravity to four dimensions, in Ref. 42 five-dimensional gauge theories have been considered on a warped



background. The action is

$$S_W^{AdS_5} = \sum_{n_\mu} \sum_{n_5=0}^{N_5-1} \left[ \frac{\beta_4}{N_c} \sum_{\mu < \nu} \text{Re Tr} \{1 - U_{\mu\nu}(n_\mu, n_5)\} + \frac{\beta_5}{N_c} \sum_{\mu} \text{Re Tr} \{1 - f(n_5) U_{\mu 5}(n_\mu, n_5)\} \right], \quad (20)$$

where  $f(n_5) = \exp(-2kn_5)$  is called the warp factor. So far Eq. (20) has been studied using the mean-field method only. The unconstrained variables  $V$  in Eq. (11) can be rescaled to absorb the warp factor in  $S_W^{AdS_5}(V)$ . A rescaling of  $H$  is then performed to keep the product  $HV$  unchanged. The resulting equations for the mean-field background with warping are similar to the ones discussed in Sec. 2.3.2 for the orbifold geometry. In Ref. 42 the phase diagram and the static potential have been studied for  $N_c = 2$ . In particular fits to the static potential have been performed and a Yukawa mass could be extracted. Close to the phase transition between the deconfined and the layered phase the shape of the static potential is consistent with a nonzero four-dimensional Yukawa mass, hinting at the existence of a Higgs phase. Earlier lattice studies of warped models in the context of gauge field localization were carried out in Ref. 43.

In Ref. 44  $SU(N_c)$  Lifshitz-type anisotropic gauge theories proposed by Hořava were discretized on the lattice. The lattice Hořava–Lifshitz action in  $D + 1$  dimensions is given by

$$S = \frac{\beta_e}{2N_c} \sum_n \sum_{i=1}^D \text{Re Tr} \{1 - U_{0i}(n)\} + \frac{\beta_g}{2N_c} \sum_n \sum_{j=1}^D \text{Re Tr} \left\{ 1 - \prod_{\substack{i=1 \\ i \neq j}}^D T_{ij}(n) \right\}, \quad (21)$$

where  $T_{ij}$  are twisted  $2 \times 1$  Wilson loops in the  $(i, j)$  plane, see Ref. 44. The “time” direction is indicated by the subscript 0 and  $i, j = 1, \dots, D$  are the spatial directions. The peculiarity of Eq. (21) is that the lattice spacing  $b$  in the temporal direction has mass dimension  $-2$  and the lattice spacing  $a$  in the spacial directions has dimension  $-1$ . The renormalization group equation at one-loop shows that the theory is asymptotically free and the continuum limit is achieved at  $\beta_e, \beta_g \rightarrow \infty$ .<sup>44</sup> First lattice simulations of the  $SU(3)$  Lifshitz-type theory present some evidence for this. There is no first order phase transition visible in the action density. The expectation values of spatial Wilson loops are found to be zero within errors consistently with the absence of a term with spatial plaquettes  $U_{ij}$  in Eq. (21).

### 3. Pure gauge theory with compact extra dimensions

In the following we summarize results from several numerical studies of the simplest non-Abelian extra-dimensional theory on the lattice, namely the  $SU(2)$  Yang–Mills theory on a five-dimensional torus with anisotropic lattice spacings,  $a_4 \neq a_5$ .<sup>20, 21, 23–26</sup> Some lattice details are introduced in Sec. 2.1. Historically, this model

with  $a_4 = a_5$  was studied in the late seventies.<sup>45</sup> It was recently extended to higher dimensions  $d > 5$  in order to test mean-field predictions.<sup>46</sup> This field of research has proven to be of great interest for a long time.

### 3.1. Phase diagram

The phase diagram of the lattice model has a rich structure that can be identified by looking at the Polyakov loop expectation values along the fifth dimension as a function of the bare parameters. Three regions can be highlighted. The location of these regions in the coupling space is summarized in Fig. 3. When all the five

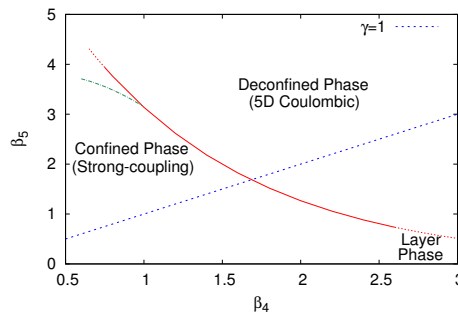


Fig. 2. A sketch of the phase diagram of the anisotropic SU(2) Yang–Mills model, taken from Ref. 47.

dimensions are large, the system undergoes a first order quantum (bulk) phase transition<sup>45</sup> separating a confined phase from a Coulomb phase (red solid line in Fig. 2).

When the fifth dimension is compactified at  $\gamma > 1$  where  $L_5 \ll L$ , this bulk phase transition becomes a second order phase transition separating a confined phase from a dimensionally reduced phase with a non-zero four-dimensional string tension and a non-zero scalar mass.<sup>24,26</sup> This phase transition line changes with  $N_5$  and corresponds to a fixed critical value of the compactification radius  $2\pi R = N_5 a_5$ . It is indicated in Fig. 2 by a green dashed-dotted line. The region with the desired separation of scales to describe a four-dimensional gauge theory with a light scalar lies just above this phase transition.

At  $\gamma < 1$ , where  $a_5 > a_4$ , a different region called *Layer phase*<sup>23,25</sup> appears as predicted by mean-field calculations.<sup>22,48</sup> In this region, the planes transverse to the fifth dimension behave as if they were decoupled from each other, indicating that degrees of freedom are localized on the four-dimensional slices. Mean-field predictions hint at a second order phase transition in this region (dotted red line in Fig. 2), but Monte Carlo simulations have not been able to conclusively determine this feature.<sup>47</sup> A similar localization mechanism was first observed for a U(1) Abelian gauge theory<sup>49–51</sup> with mean-field and Monte Carlo methods: the potential

along  $d = 4$  hyperplanes is Coulombic, why it is confining in the bulk, constraining fields to fluctuate only in four-dimensions. Another idea, that achieves localization, relies on topological defects, like a domain wall, and was demonstrated in Ref. 52: a confining potential in the bulk becomes deconfining on the defect, where a theory with a reduced gauge symmetry group is realized. An exploratory lattice study was carried over in Ref. 53.

To conclude, the phase diagram of the  $d = 5$  SU(2) Yang–Mills theory on the lattice does not contain a second order phase transition or a critical point where a five-dimensional continuum theory can be defined non-perturbatively (contrary to expectations from the  $\epsilon$ -expansion<sup>54,55</sup>). However, regions of parameters where the theory dynamically reduces from five to four dimensions exist at  $\gamma > 1$  and  $\gamma < 1$ .

This phase diagram study has been extended to the larger gauge group of SU(3) in Ref. 56 and Ref. 57. The reader should refer to those references for further details.

### 3.2. Spectrum and static potential

The nature of the dimensionally reduced theory can be checked with non-perturbative calculations of the spectrum and of the static potential.

At  $\gamma > 1$ , the system is characterized by three energy scales  $\Lambda_{UV} \approx \frac{1}{a_4}$ ,  $\Lambda_R \approx \frac{1}{N_5 a_5}$  and  $m_5$ , pictorially shown in Fig. 1. They were calculated for various values of the bare parameters of the lattice model  $\beta_4$ ,  $\beta_5$  and  $N_5$  (in the large- $N_4$  limit)<sup>24,26</sup> in units of the four-dimensional lattice spacing, before rescaling them in units of the four-dimensional string tension. In other words, the lattice model can now be described in terms of what a four-dimensional observer would measure: the string tension  $\sqrt{\sigma}$  is the inverse of the characteristic length in  $d = 4$ . Clearly this information is sufficient to check if the picture of Fig. 1 holds non-perturbatively.

Technically, the measurement of the four-dimensional string tension in units of the lattice spacing,  $a_4 \sqrt{\sigma}$ , is done utilizing temporal correlation functions of spatial Polyakov loops (averaged over the fifth dimension). The measurement of the scalar mass, again in units of the lattice spacing,  $a_4 m_5$ , is instead performed using correlators of different types of four-dimensional scalar interpolating operators. For example, a scalar operator from the four-dimensional point of view is the Polyakov loop wrapping around the fifth dimension. Another scalar operator in a four-dimensional gauge theory is a glueball operator (a rotationally invariant combination of closed Wilson paths in three dimensions). They both carry scalar quantum numbers but the first is intrinsically related to the extra-dimensional nature of the system. Using both types of scalar operators is useful in disentangling extra-dimensional contributions to the scalar spectrum. A careful study of the scalar spectrum for a specific set of lattice parameters is reported in Ref. 26 and the validity of Eq. (1) in the non-perturbative regime is confirmed.

At  $\gamma < 1$ , in the layer phase, the static potential was studied numerically<sup>25</sup> to check the mean-field prediction<sup>48</sup> that  $d = 4$  hyperplanes decouple, giving rise to an effective dimensionally reduced SU(2) Yang–Mills theory plus an adjoint scalar.

12 *F. Knechtli and E. Rinaldi*

The static potential along the hyperplanes orthogonal to the fifth dimension is compatible with a four-dimensional description<sup>25</sup> along the bulk phase transition line, but still in the confined phase ( $\beta_5 < \beta_5^{\text{crit}}$ ). Moreover, the temporal Polyakov loops, in the phase where they have a non-zero expectation value, fluctuate independently depending on which  $d = 4$  hyperplane they originate from: at each  $x_5$  coordinate along the extra dimension they have different central values. Both these observations support the notion that dimensional reduction happens at  $\gamma < 1$  due to a localization mechanism along the  $d = 4$  hyperplanes.

### 3.3. Dimensional reduction and continuum limit

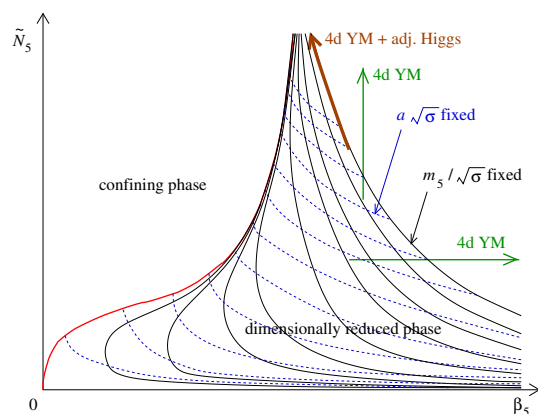


Fig. 3. A sketch of the lines of constant physics for the anisotropic SU(2) Yang–Mills model, taken from Ref. 24.

The non-perturbative studies of the scalar mass and of the static potential for the anisotropic SU(2) Yang–Mills model are useful to determine the effective dimensionally-reduced description of the theory in different regions of the phase diagram, and the corresponding lines of constant physics. Without lattice calculations, these lines can only be guessed with perturbative predictions and may miss important non-perturbative contributions.<sup>58</sup>

The region at  $\gamma > 1$  has been studied with great details and accuracy by different groups.<sup>24–26</sup> A sketch summarizing the results, taken from Ref. 24, is reported in Fig. 3. The figure shows a phase diagram in the  $(\beta_5, \tilde{N}_5)$  plane (cfr. Sec. 2.1) where a phase transition line of second order separates the confined phase from the dimensionally reduced phase where  $L_5$  is small, as described in Sec. 3.1.

The dashed lines on the right of the phase transition describe the perturbative behavior of a constant four-dimensional string tension and were checked non-perturbatively.<sup>24,26</sup> Similarly, the solid lines represent constant  $m_5/\sqrt{\sigma}$ , again following a perturbative expectation that had been checked with lattice numerical methods.<sup>24,26</sup>

A line of constant scalar mass  $m_5$  in units of the four-dimensional theory  $\sqrt{\sigma}$  represents a Yang–Mills theory with an adjoint scalar field. Along this line, the cutoff is removed by going to larger  $\tilde{N}_5$  values: the separation between the cutoff and the compactification scale increases. The scalar particle can be light or heavy depending on the size of the extra dimension, with the lightest one being closest to the phase transition line (where the correlation length  $1/m_5$  diverges). Any direction but the one along a constant  $m_5/\sqrt{\sigma}$  line results in a pure  $d = 4$  Yang–Mills theory when the cutoff is removed. This can be easily seen because lines with heavier  $m_5/\sqrt{\sigma}$  are crossed in doing so: the scalar field decouples and can be integrated out. This is consistent with the naïve non-renormalizability of a five-dimensional theory: removing the cutoff always yield a four-dimensional Yang–Mills theory in the dimensionally-reduced phase.

The direction at constant  $\tilde{N}_5$  was explicitly checked non-perturbatively in Ref. 26: the lightest scalar of the theory becomes a glueball state as  $\beta_5$  is increased and the scalar coming from compactification is pushed to higher energies. A striking feature of this phase diagram, which is perhaps unexpected, is that the theory is also a four-dimensional Yang–Mills theory along the direction at fixed  $\beta_5$  (as long as the phase transition is avoided.) This direction corresponds to increasingly large compactification radius in units of the four-dimensional cutoff. The theory we end up with does not know about its extra-dimensional origin, even when the extra dimension is large: this approach to dimensional reduction was already suggested in the framework of D-theories.<sup>56,59,60</sup>

### 3.4. Mean-field results on the torus

The investigation of the lattice phase diagram with Monte Carlo methods was inspired by mean-field calculations described in Sec. 2.3. The mean-field expansion has been applied to the anisotropic SU(2) gauge theory on a periodic lattice in five dimensions in Refs. 22, 48. The extension of the calculation to SU( $N_c$ ) was done in Ref. 61.

The mean-field phase diagram has three phases: a confined phase, where the background vanishes everywhere; a deconfined phase, where the background is non-zero everywhere; and a layered phase, where the background vanishes along the fifth dimension and is nonzero elsewhere. In Ref. 22, by analyzing the shape of the static potential, two regions were identified, where dimensional reduction occurs. One region is for the anisotropy parameter in Eq. (2)  $\gamma \gg 1$  and it corresponds to a compact extra dimension. The other region is for  $\gamma < 1$  close to the phase transition into the layered phase. For sufficiently small  $\gamma < 1$  the phase transition, as seen by the mean-field, turns from first to second order. When it is of second order a continuum limit can be taken. In this case, dimensional reduction by localization on the four-dimensional slices orthogonal to the extra dimension was shown in Ref. 48. Although Monte Carlo studies did not confirm the existence of a second order phase transition, they show hints for dimensional reduction through localization at

14 *F. Knechtli and E. Rinaldi*

$\gamma < 1$ .<sup>25</sup>

The mean-field expansion is expected to work better when the number of dimensions  $d$  is increased. On the isotropic torus the critical value  $\beta_c^{\text{MF}}$  separates the confined from the Coulomb phase. An interesting observation was made in Ref. 46. The combination  $(d - 1)\beta_c^{\text{MF}}$  which fulfills Eq. (19) is independent on the number of dimensions  $d$ . This leads to the relation

$$(d - 1)\beta_c^{\text{MF}} \simeq 6.704840. \quad (22)$$

This relation is compared to the location of the phase transition from Monte Carlo simulations in  $d = 5, 6, 7, 8$  and shows a nice agreement.

#### 4. The Hosotani mechanism on the lattice

The Hosotani mechanism<sup>11,62</sup> has been established only in perturbation theory, where an effective potential  $V_{\text{eff}}(\theta_{\text{H}})$  can be calculated for the Aharonov-Bohm phase  $\theta_{\text{H}}$ , whose fluctuations correspond to the Higgs mass, and remains free of divergences at one loop. This spontaneous symmetry breaking mechanism that gives rise to the Higgs and vector boson masses in the extra-dimensional formalism was confirmed non-perturbatively with lattice field theory methods in Ref. 63.

Different realizations of gauge symmetry breaking described by the Hosotani mechanism, correspond to different minima in  $V_{\text{eff}}(\theta_{\text{H}})$ . The minima of the effective potential are located at different values of  $\theta_{\text{H}}$  which are probed by looking at the expectation value of the Polyakov loop in the compact direction  $y$ :

$$W(x) = P \exp \left( ig \int_0^{2\pi R} dy A_y(x, y) \right), \quad (23)$$

where  $g$  is the gauge coupling constant and  $A_y(x, y)$  the gauge potential in the compact direction with radius  $R$ . The eigenvalues of  $W(x)$ , denoted by  $\{e^{i\theta_1}, e^{i\theta_2}, e^{i\theta_3}\}$ , are the elements of the Aharonov-Bohm phase in the compact dimension and represent the dynamical degrees of freedom which will become the longitudinal components of the vector boson fields and of the Higgs field in a complete Gauge-Higgs Unification scenario.

Ref. 63 studied the phase diagram of a  $(3 + 1)$ -dimensional  $\text{SU}(3)$  lattice gauge theory with fermions in the adjoint (ad) and in the fundamental (fd) representation with a compact direction. The Hosotani mechanism works generically with any space-time dimensionality, and this lattice theory is simpler to study than its five-dimensional counterpart (due to the inherent difficulty of formulating discretized versions of the fermionic algebra in extra dimensions). The minima of  $V_{\text{eff}}(\theta_{\text{H}})$  are investigated non-perturbatively in this setup.

The lattice version of Eq. (23), denoted by  $P_3$ , and its adjoint counterpart,  $P_8$ , are computed for different values of gauge coupling  $\beta$  and fermion masses  $m_{\text{fd}}$ ,  $m_{\text{ad}}$ , as well as different boundary conditions  $\alpha_{\text{fd}}$  for the fundamental fermions in the

compact direction. The distribution of eigenvalues of  $P_3$  is compared to the values of  $\theta_H = (\theta_1, \theta_2, \theta_3)$  at the minima of the perturbative one-loop effective potential.

Let us focus on the case where the SU(3) gauge theory is coupled to two massive adjoint fermions with periodic boundary conditions on the toroidal lattice.<sup>64</sup> By looking at the expectation value of  $P_3$ , one can identify four different phases at fixed  $m_{\text{ad}}$  as the extra dimension size decreases by increasing  $\beta$ : they are called, in order, X, A, B and C. Perturbatively, different phases are related to different configurations of the minima of  $V_{\text{eff}}(\theta_H)$  and they appear as the product  $m_{\text{ad}}R$  gets smaller.

The *X phase* corresponds to a confined SU(3) symmetric phase which disappears when the extra dimension starts to shrink. The *A phase* corresponds to a degenerate triplet of minima for the effective potential:  $P_3$  takes the values of the cubic root of unity with equal probability and the  $\theta_i$  eigenvalues are always degenerate for each case (modulo the Haar measure). This phase is deconfined, but still SU(3) symmetric. If one keeps driving  $R$  to zero, the *B phase* appears (called *split* in the original study<sup>64</sup>): in terms of the Hosotani mechanism, this phase corresponds to the SU(3) gauge symmetry being broken to  $SU(2) \times U(1)$  and this can be seen by investigating the eigenvalues  $\theta_i$ . Again there is a triplet of minima where two elements of  $\theta_H$  are degenerate while the third is different. At last, the *C phase*, originally called *reconfined*,<sup>64</sup> has  $\langle P_3 \rangle = 0$ , but it corresponds to a  $U(1) \times U(1)$  gauge symmetry, where the eigenvalues  $\theta_i$  take maximally displaced values:  $(0, \frac{2}{3}\pi, -\frac{2}{3}\pi)$ . In the *B* and *C phases*, the masses of the adjoint scalars are calculated by looking at the fluctuations around the minima of the potential and they agree with the perturbative predictions.

The correspondence between the perturbative Hosotani mechanism and the non-perturbative phases on the lattice was also checked for the case of a SU(3) gauge theory with four fundamental fermions by changing their temporal boundary conditions. However, these studies have not attempted to investigate if this correspondence survives in the continuum limit of the lattice theory.

It is interesting to note that the lattice phase diagrams for the two theories described above were originally investigated for reasons that are not related to the Hosotani mechanism. The theory with adjoint fermions was studied in Ref. 64 to study volume independence in the orientifold planar equivalence.<sup>65</sup> On the other hand, different boundary conditions for fundamental fermions were studied in the context of finite density QCD with imaginary chemical potential.<sup>66</sup>

A first study of a four-dimensional theory, where spontaneous symmetry breaking is induced by the Hosotani mechanism in five dimensions, was performed in Ref. 67. An external potential  $h_{\text{fd}}\text{Re}(\text{Tr}P_5) + h_{\text{ad}}|\text{Tr}P_5|^2$ , based on the Polyakov loop in the extra dimension  $P_5$ , is used to mimic the presence of adjoint fermions and break the gauge symmetry. In the vacuum where the gauge symmetry group is  $U(1) \times U(1)$  (cfr. the C phase above), a topological excitation which is gauge invariant only under a U(1) group, namely an Abelian flux, is found to be stable, while it would immediately disappear when the full SU(3) gauge symmetry is restored by

switching off the external potential.

## 5. Non-perturbative gauge-Higgs unification

The phenomenological interest in orbifold theories relies on the possibility to break spontaneously the boundary gauge group  $H$  (see Sec. 2.2) and doing so to reproduce the Higgs mechanism of the Standard Model. Perturbative calculations of the effective potential for the extra-dimensional scalar indicate that spontaneous symmetry breaking cannot occur unless fermions are included, see Ref. 68. The perturbative limit of these theories is trivial and one wonders about the situation in the non-perturbative regime. The findings of the earlier Monte Carlo studies of the  $SU(2)$  pure gauge theory on the orbifold<sup>33,69</sup> showed indeed evidence for a massive gauge boson.

### 5.1. Mean-field results on the orbifold

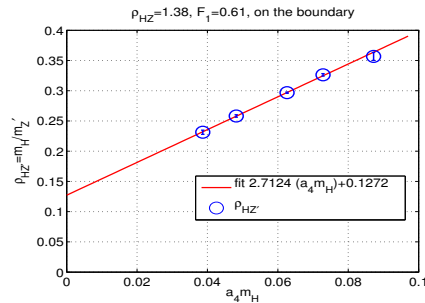


Fig. 4. The ratio  $\frac{m_H}{m_{Z'}}$  computed in mean-field on the orbifold. From Ref. 70.

A first attempt to probe analytically five-dimensional gauge theories on the orbifold away from the trivial perturbative limit was made in Ref. 29. Including the effects of a finite lattice spacing in the Coleman-Weinberg computations<sup>71</sup> of the effective potential leads to the possibility of spontaneous symmetry breaking in the pure gauge theory, contrary to the expectation based on perturbative calculations<sup>68</sup> but in accordance with the Monte Carlo results<sup>33,69</sup>. A further verification of the existence of spontaneous symmetry breaking was provided by the mean-field calculations in Refs. 38, 70. The scalar mass is extracted from the correlator of scalar Polyakov loops. The gauge boson mass is obtained by determining a four-dimensional Yukawa mass from the static potential.<sup>38</sup> It turns out to be non-zero on the orbifold in the limit of an infinitely large boundary, which is the evidence for the spontaneous breaking of the boundary  $U(1)$  gauge symmetry. The same mass extracted on the torus vanishes instead.

At sufficiently small  $\gamma$  it is possible to construct lines of constant physics in the deconfined phase, where the mean-field background is non-zero everywhere. The



lines are close to the phase boundary and in the regime where the phase transition is of second order according to the mean-field. In Ref. 70 such a line is constructed where the Higgs to  $Z$  boson ratio is kept fixed to  $\rho \equiv \frac{m_H}{m_Z} = 1.38$  and the Higgs mass is kept fixed to  $F_1 = m_H R = 0.61$ , where  $\pi R$  is the size of the extra dimension. From the boundary static potential it is possible to extract also a higher Yukawa mass which corresponds to an excited  $Z'$  boson state. Fig. 4 shows the continuum extrapolation of the ratio  $\frac{m_H}{m_{Z'}}$ . For  $m_Z = 91.19 \text{ GeV}$  the result is a  $Z'$  mass of 989 GeV. We notice that the fact that the ratio shown Fig. 4 can be extrapolated also implies the finiteness of the Higgs mass.

## 5.2. Monte Carlo results on the orbifold

The latest Monte Carlo results, which are favorably pointing towards the suitability of this theory for describing the electro-weak sector of the Standard Model are reported in Ref. 72, of which this section is a summary.

### 5.2.1. Phase diagram

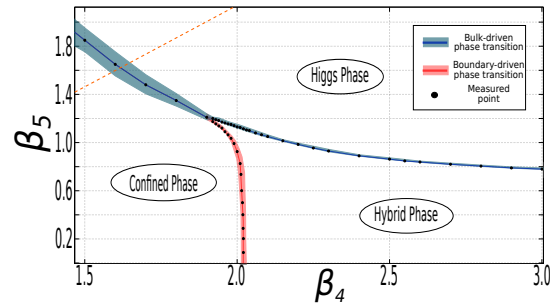


Fig. 5. The phase diagram of the five-dimensional anisotropic orbifold ( $N_5 = 4$ ) in the region of the Higgs-hybrid phase transition. From Ref. 72.

In Ref. 72, a five-dimensional  $SU(2)$  theory was studied on an anisotropic lattice. On the boundaries, where the "Standard Model-like" physics would be found, the gauge group reduces to  $U(1)$  due to the orbifold geometry. The study of this model is intended as a proof of principle: the investigation of a larger model which would contain, on the boundary, the entirety of the Higgs sector will follow once the theory has been shown to be viable.

The system has been found to exhibit three phases, characterized by the expectation value of the Polyakov loop: in the confined (de-confined) phase the Polyakov loop exhibit zero (non-zero) expectation value in every direction. In this context, the de-confined phase is labelled Higgs phase, because it is where the Higgs potential develops SSB, giving rise to non-zero gauge boson masses. The third phase,

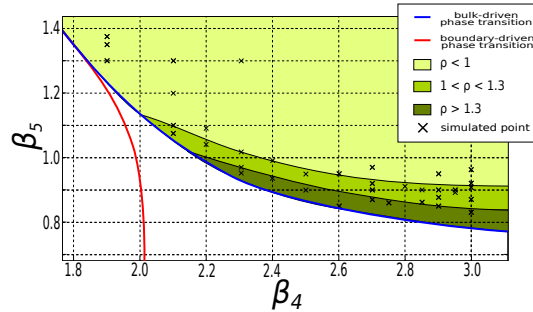
18 *F. Knechtli and E. Rinaldi*


Fig. 6. The ratio  $\frac{m_H}{m_Z}$  on the orbifold. The different shadings of green correspond to  $\rho < 1$  (lightest shade),  $1 \leq \rho \leq 1.3$  (middle shade) and  $\rho > 1.3$  (darkest shade). From Ref. 72.

which is characteristic only of the orbifold geometry, shows confined dynamics in the orbifold's bulk, and de-confined dynamics on its boundaries; it is, therefore, called hybrid phase. Both phase transitions have been found to be first order for all explored parameter values. The phase diagram in the  $(\beta_4, \beta_5)$  plane for the orbifold with  $N_5 = 4$  is shown in Fig. 5. The Figure shows the region where the bare anisotropy  $\gamma \leq 1$ . The phase transition line separating the confined and the hybrid phases originates from the phase transition of the four-dimensional U(1) theory on the orbifold boundaries. Its appearance is crucial because it changes the properties of the spectrum in the Higgs phase, as we describe below.

### 5.2.2. Spectrum and the Higgs mechanism

Although the Higgs mechanism is active everywhere in the Higgs phase, the mass measurements of the scalar and vector boson (which we identify with the  $Z$  boson, due to the quantum numbers of the operators we use) suggest that only a smaller region of the parameter space is capable of reproducing the physics of the Standard Model. Fig. 6 shows the observed value of the ratio  $\rho \equiv \frac{m_H}{m_Z}$  on top of the theory's phase diagram: the region in proximity of the Higgs-hybrid phase transition is where  $\rho$  approaches the physical value of 1.37.

### 5.2.3. Dimensional reduction by localization

Exactly in the same region, where the masses of the Higgs and  $Z$  boson show the physical ratio, dimensional reduction is observed. As shown in Fig. 7, the static potential measured on the boundary (left panel) at  $(\beta_4 = 2.1, \beta_5 = 1.075, N_5 = 4)$  is of four-dimensional type, whereas the same observable measured in the orbifold's bulk (right panel) is clearly five-dimensional. Moreover, the mass of the  $Z$  boson, which can be extracted from the fit to the four-dimensional Yukawa potential, has been found to be in perfect agreement with the mass measured in the same point through spectroscopic calculations. Contrastingly, in the region further away from the phase transition, where the hierarchy of the masses is unphysical, no hint of

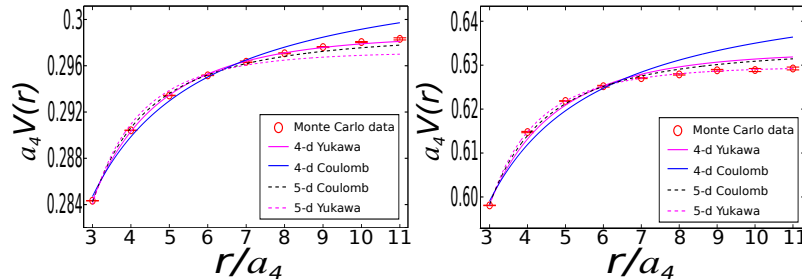


Fig. 7. The static quark-antiquark potential on the orbifold measured on the boundary (left) and in the bulk (right) in proximity of the Higgs-hybrid phase transition. From Ref. 72.

four-dimensional physics could be observed neither on the orbifold's boundaries nor in the bulk.

On the other side of the phase transition, in the hybrid phase, the static potential is found to be four dimensional on all space-time layers. The  $U(1)$  boundaries exhibit de-confined physics, consistently with the behaviour of a pure 4-d  $U(1)$  theory at a matching value of the coupling  $\beta = \frac{\beta_4}{2}$ .<sup>73</sup> On the other hand, the  $SU(2)$  bulk layers show confinement. Although this phase is not of immediate interest in the study of the Higgs mechanism, as it does not possess SSB, a deeper knowledge of what happens in it could prove a useful tool in understanding processes in the Higgs phase.

While all the results presented here have been obtained on  $N_5 = 4$  lattices, measurements on  $N_5 > 4$  have shown no qualitative difference from those quoted, the only change being that the masses become lighter in lattice units and the region of the phase diagram where the physical mass hierarchy is found become slightly larger. This suggests, consistently with the idea of localization, that the extent of the extra dimension plays only a minor role in the resulting physics.

#### 5.2.4. Effective theory and the Higgs mechanism

Global symmetries are essential for the Higgs mechanism to take place in the non-perturbative gauge invariant formulation of the theory on the lattice. Elitzur's theorem dictates that any physical effect associated with the breaking of a local symmetry must originate from the spontaneous breaking of a non-trivial global symmetry.<sup>18</sup>

In Refs. 35, 72 it is shown that the spontaneous breaking of the boundary gauge symmetry  $H$  on the orbifold is governed by the stick symmetry<sup>34</sup>  $\mathcal{S} = \mathcal{S}_L \cdot \mathcal{S}_R$  defined in Eqs. (9) and (10). The order parameter is the vector Polyakov loop defined in Eq. (8), which is odd under the stick symmetry  $\mathcal{S}$  and from which a nonzero gauge boson mass can be determined. The center symmetry is obtained by applying twice the stick symmetry. The scalar and vector Polyakov loops on the orbifold are invariant under the center symmetry (unlike on the torus). As a result,

the spontaneous breaking of the stick symmetry does not trigger finite temperature phase transitions but a Higgs-mechanism like phase transition.

The stick symmetry appears to be valid only at finite lattice spacing.<sup>72</sup> In the perturbative continuum limit the symmetry disappears. This explains the absence of spontaneous symmetry breaking in pure gauge perturbative models of gauge-Higgs unification.<sup>68</sup> In non-perturbative gauge-Higgs unification the spontaneous breaking of the stick symmetry and the resulting Higgs mechanism make sense only as an effective theory. The construction of lines of constant physics which describe the effective theory in a finite range of lattice spacings is work in progress. If they can be constructed, they will be a proof of the (non-perturbative) finiteness of the Higgs mass. In addition, they will predict the energy of the excited states of the Higgs and gauge boson particles to be compared with experimental results.

## 6. Perspectives

Extra-dimensional models are actively being searched for at the LHC. Non-perturbative investigations using lattice field theory methods, described in this review, have proven successful in testing several scenarios relevant for gauge-Higgs unification. Despite the long history of numerical simulations for extra-dimensional models, there is still no complete description that is directly applicable to phenomenology. Some of the main reasons for this are listed in the following. They should be used as a reference guide for future works aimed at improving our understanding of phenomenologically relevant extra-dimensional models.

Lattice models with one or more extra dimensions are inherently more expensive in terms of computing cost, and the same is true for larger gauge groups which are needed to embed the electro-weak sector of the Standard Model. Moreover, it is technically challenging to define discretized versions of the fermionic algebra when the number of space-time dimensions is not even. Furthermore, it seems that a non-trivial continuum limit of extra-dimensional gauge theories is hard to achieve. Even if such a limit does not exist, lines of constant physics can be constructed when lattice models are interpreted as effective field theory descriptions with an ultraviolet cutoff. There are investigations of alternative gauge theories where a continuum limit in higher dimension might exist. More sophisticated extra-dimensional models are based on a warped metric and lattice studies consider also these models.

To conclude, we think that this is a very active field and will see significant advances in the future.

## Acknowledgments

We thank N. Irges and G. Cossu for useful comments. F. K. acknowledges the support of the Deutsche Forschungsgemeinschaft (DFG) under contract KN 947/1-2. E. R. acknowledges the support of the DOE under contract DE-AC52-07NA27344 (LLNL).

## References

1. ATLAS Collaboration Collaboration (G. Aad *et al.*), *Phys.Lett.* **B716**, 1 (2012), 1207.7214.
2. CMS Collaboration Collaboration (S. Chatrchyan *et al.*), *Phys.Lett.* **B716**, 30 (2012), 1207.7235.
3. F. Englert and R. Brout, *Phys.Rev.Lett.* **13**, 321 (1964).
4. P. W. Higgs, *Phys.Lett.* **12**, 132 (1964).
5. P. W. Higgs, *Phys.Rev.Lett.* **13**, 508 (1964).
6. CMS Collaboration, Search for new physics in high mass diphoton events in proton-proton collisions at  $\sqrt{s} = 13$  TeV, in *ATLAS and CMS physics results from Run 2, CERN, 15 December*, (2015).
7. ATLAS Collaboration, Search for resonances decaying to photon pairs in  $3.2 \text{ fb}^{-1}$  of  $pp$  collisions at  $\sqrt{s} = 13$  TeV with the ATLAS detector, in *ATLAS and CMS physics results from Run 2, CERN, 15 December*, (2015).
8. T. Kaluza, *Sitzungsber.Preuss.Akad.Wiss.Berlin (Math.Phys.)* **1921**, 966 (1921).
9. O. Klein, *Z.Phys.* **37**, 895 (1926).
10. N. Manton, *Nucl.Phys.* **B158**, 141 (1979).
11. Y. Hosotani, *Phys. Lett.* **B126**, 309 (1983).
12. H. Hatanaka, T. Inami and C. S. Lim, *Mod. Phys. Lett.* **A13**, 2601 (1998), hep-th/9805067.
13. H.-C. Cheng, K. T. Matchev and M. Schmaltz, *Phys. Rev.* **D66**, 036005 (2002), hep-ph/0204342.
14. G. von Gersdorff, N. Irges and M. Quiros, *Nucl. Phys.* **B635**, 127 (2002), hep-th/0204223.
15. Y. Hosotani (2005), hep-ph/0504272.
16. Y. Hosotani, N. Maru, K. Takenaga and T. Yamashita, *Prog. Theor. Phys.* **118**, 1053 (2007), 0709.2844.
17. L. Del Debbio, E. Kerrane and R. Russo, *Phys. Rev.* **D80**, 025003 (2009), 0812.3129.
18. S. Elitzur, *Phys.Rev.* **D12**, 3978 (1975).
19. Y. Fu and H. B. Nielsen, *Nucl.Phys.* **B236**, 167 (1984).
20. S. Ejiri, J. Kubo and M. Murata, *Phys. Rev.* **D62**, 105025 (2000), hep-ph/0006217.
21. S. Ejiri, S. Fujimoto and J. Kubo, *Phys.Rev.* **D66**, 036002 (2002), hep-lat/0204022.
22. N. Irges and F. Knechtli, *Nucl. Phys.* **B822**, 1 (2009), 0905.2757.
23. K. Farakos and S. Vrentzos, *Nucl.Phys.* **B862**, 633 (2012), 1007.4442.
24. P. de Forcrand, A. Kurkela and M. Panero, *JHEP* **06**, 050 (2010), 1003.4643.
25. F. Knechtli, M. Luz and A. Rago, *Nucl.Phys.* **B856**, 74 (2012), 1110.4210.
26. L. Del Debbio, A. Hart and E. Rinaldi, *JHEP* **1207**, 178 (2012), 1203.2116.
27. S. Ejiri, Y. Iwasaki and K. Kanaya, *Phys. Rev.* **D58**, 094505 (1998), hep-lat/9806007.
28. K. R. Dienes, E. Dudas and T. Gherghetta, *Nucl. Phys.* **B537**, 47 (1999), hep-ph/9806292.
29. N. Irges, F. Knechtli and M. Luz, *JHEP* **0708**, 028 (2007), 0706.3806.
30. N. Irges and F. Knechtli, *Nucl. Phys.* **B719**, 121 (2005), hep-lat/0411018.
31. F. Knechtli, B. Bunk and N. Irges, *PoS LAT2005*, 280 (2006), hep-lat/0509071.
32. A. Hebecker and J. March-Russell, *Nucl.Phys.* **B625**, 128 (2002), hep-ph/0107039.
33. N. Irges and F. Knechtli, *Nucl. Phys.* **B775**, 283 (2007), hep-lat/0609045.
34. K. Ishiyama, M. Murata, H. So and K. Takenaga, *Prog.Theor.Phys.* **123**, 257 (2010), 0911.4555.
35. N. Irges and F. Knechtli, *JHEP* **1406**, 070 (2014), 1312.3142.
36. J.-M. Drouffe and J.-B. Zuber, *Phys.Rept.* **102**, 1 (1983).
37. W. Rühl, *Z. Phys.* **C18**, 207 (1983).

22 *F. Knechtli and E. Rinaldi*

38. N. Irges, F. Knechtli and K. Yoneyama, *Nucl.Phys.* **B865**, 541 (2012), 1206.4907.
39. F. Knechtli, The Static potential in the SU(2) Higgs model, PhD thesis, Humboldt U., Berlin (1999).
40. L. Randall and R. Sundrum, *Phys. Rev. Lett.* **83**, 3370 (1999), hep-ph/9905221.
41. L. Randall and R. Sundrum, *Phys. Rev. Lett.* **83**, 4690 (1999), hep-th/9906064.
42. R. D. Kenway and E. Lambrou, Five-dimensional Gauge Theories in a warped background, in *Proceedings, 33rd International Symposium on Lattice Field Theory (Lattice 2015)*, (2015). 1510.07601.
43. M. Laine, H. B. Meyer, K. Rummukainen and M. Shaposhnikov, *JHEP* **01**, 068 (2003), hep-ph/0211149.
44. T. Kanazawa and A. Yamamoto, *Phys. Rev.* **D91**, 074508 (2015), 1411.4667.
45. M. Creutz, *Phys. Rev. Lett.* **43**, 553 (1979).
46. N. Irges, G. Koutsoumbas and K. Ntrekis, *Phys. Rev.* **D92**, 094506 (2015), 1503.06431.
47. L. Del Debbio, R. D. Kenway, E. Lambrou and E. Rinaldi, *Phys. Lett.* **B724**, 133 (2013), 1305.0752.
48. N. Irges and F. Knechtli, *Phys.Lett.* **B685**, 86 (2010), 0910.5427.
49. P. Dimopoulos, K. Farakos and S. Vrentzos, *Phys. Rev.* **D74**, 094506 (2006), hep-lat/0607033.
50. K. Farakos and S. Vrentzos, *Phys. Rev.* **D77**, 094511 (2008), 0801.3722.
51. K. Farakos and S. Vrentzos, *Phys. Rev.* **D78**, 114502 (2008), 0807.3463.
52. G. R. Dvali and M. A. Shifman, *Nucl. Phys.* **B504**, 127 (1997), hep-th/9611213.
53. M. Laine, H. Meyer, K. Rummukainen and M. Shaposhnikov, *JHEP* **0404**, 027 (2004), hep-ph/0404058.
54. H. Gies, *Phys. Rev.* **D68**, 085015 (2003), hep-th/0305208.
55. T. R. Morris, *JHEP* **01**, 002 (2005), hep-ph/0410142.
56. B. B. Beard *et al.*, *Nucl. Phys. Proc. Suppl.* **63**, 775 (1998), hep-lat/9709120.
57. E. Itou, K. Kashiwa and N. Nakamoto (2014), 1403.6277.
58. E. Rinaldi, Non-perturbative aspects of physics beyond the Standard Model, PhD thesis, Edinburgh U. (2013).
59. S. Chandrasekharan and U. J. Wiese, *Nucl. Phys.* **B492**, 455 (1997), hep-lat/9609042.
60. R. Brower, S. Chandrasekharan and U. Wiese, *Phys.Rev.* **D60**, 094502 (1999), hep-th/9704106.
61. N. Irges and G. Koutsoumbas, *JHEP* **08**, 103 (2012), 1205.0379.
62. Y. Hosotani, *Phys.Lett.* **B129**, 193 (1983).
63. G. Cossu, H. Hatanaka, Y. Hosotani and J.-I. Noaki, *Phys.Rev.* **D89**, 094509 (2014), 1309.4198.
64. G. Cossu and M. D’Elia, *JHEP* **07**, 048 (2009), 0904.1353.
65. P. Kovtun, M. Unsal and L. G. Yaffe, *JHEP* **06**, 019 (2007), hep-th/0702021.
66. P. de Forcrand and O. Philipsen, *Nucl. Phys.* **B642**, 290 (2002), hep-lat/0205016.
67. O. Akerlund and P. de Forcrand, *PoS LATTICE2014*, 272 (2015), 1503.00429.
68. M. Kubo, C. Lim and H. Yamashita, *Mod.Phys.Lett.* **A17**, 2249 (2002), hep-ph/0111327.
69. N. Irges and F. Knechtli (2006), hep-lat/0604006.
70. N. Irges, F. Knechtli and K. Yoneyama, *Phys.Lett.* **B722**, 378 (2013), 1212.5514.
71. I. Antoniadis, K. Benakli and M. Quiros, *New J.Phys.* **3**, 20 (2001), hep-th/0108005.
72. M. Alberti, N. Irges, F. Knechtli and G. Moir, *JHEP* **09**, 159 (2015), 1506.06035.
73. G. Arnold, B. Bunk, T. Lippert and K. Schilling, *Nucl.Phys.Proc.Suppl.* **119**, 864 (2003), hep-lat/0210010.